COMMUNICATIONS

Ab initio studies of quasi-one-dimensional pentagon and hexagon ice nanotubes

J. Bai
Department of Chemistry and Physics, University of Nebraska, Lincoln, Nebraska 68588

C.-R. Su
Department of Physics and Center for Atomic and Molecular Nanosciences, Tsinghua University, Beijing, 100084, China

R. D. Parra
Department of Chemistry, DePaul University, Chicago, Illinois 60604

X. C. Zeng[a)]
Department of Chemistry, University of Nebraska, Lincoln, Nebraska 68588

H. Tanaka
Department of Chemistry, Okayama University, Okayama 700-8530, Japan

K. Koga
Department of Chemistry, Cornell University, Ithaca, New York 14853

J.-M. Li
Department of Physics and Center for Atomic and Molecular Nanosciences, Tsinghua University, Beijing, 100084, China

(Received 13 November 2002; accepted 3 January 2003)

Ab initio plane-wave total-energy calcuation is carried out to study the relative stability of the quasi-one-dimensional (Q1D) pentagon and hexagon ice nanotubes. Electronic structure calculations indicate the two Q1D ice nanotubes have nearly the same band structures and energy bandgap as those of proton-ordered bulk ice I_h. *Ab initio* molecular-orbital and density-functional theory calculations, as well as three classical potential models of water, are also employed to investigate the relative stability of the pentagon and hexagon water clusters $(H_2O)_{30}$, $(H_2O)_{60}$, and $(H_2O)_{120}$. Clusters of this kind can serve to bridge the gap between the small polygonal water rings and the infinitely long Q1D polygon ice nanotubes. It is found that the polygon water prisms with the size $(H_2O)_{120}$ begin to show the relative energetic behavior of the infinitely long polygon ice nanotubes. © *2003 American Institute of Physics.* [DOI: 10.1063/1.1555091]

Ab initio computer simulations[1] can explore regions of phase diagram not easily accessible by laboratory experiments. For example, the first direct observation of phase transformation of the densest ice phase (among thirteen crystalline phases of ice), ice X, was established from *ab initio* molecular dynamics simulation,[2] whereas the experimental evidence of existence of the ice X is thus far only inferred from spectroscopy.[3] Recently, classical molecular mechanics[4,5] and molecular dynamics simulations[6,7] of water encapsulated in carbon nanotubes have been reported, which suggests possible existence of four quasi-one-dimensional (Q1D) polymorphs of ice nanotube. Among these Q1D polymorphs, pentagon and hexagon ice nanotubes are the two most stable ones.[4] In the previous studies, the TIP4P potential of water[8] has been used. Since the potential is derived from fitting to experimental data for bulk water, extension of the potential to highly confined water may be only qualitative or semiquantitative. Thus, the predicted polymorphs of Q1D ice remains to be confirmed, at least by more quantitative means, although direct experimental observation of these phases is the ultimate confirmation.[9] In this communication, we report results of *ab initio* pseudopotential total-energy calculation to further affirm the existence of polymorphs of Q1D ice nanotube. Our calculations show that both hexagon and pentagon ice nanotubes are metastable solid phase in vacuum at 0 K and they are nearly isoenergetic. Moreover, calculation of the electron density of states indicated that the two Q1D polymorphs have nearly the same energy bandgap as the proton-ordered bulk ice I_h. Finally, relative stability of the finite-size pentagon and hexagon water clusters at 0 K is also examined using all-electron quantum chemistry methods as well as three additional classical potential models of water.

For Q1D ice nanotubes, we used the Cambridge Serial Total Energy Package (CASTEP)[10] to calculate the total energy per molecule and forces within the framework of density-functional theory (DFT). The exchange-correlation

a)Electronic mail: xzeng1@unl.edu

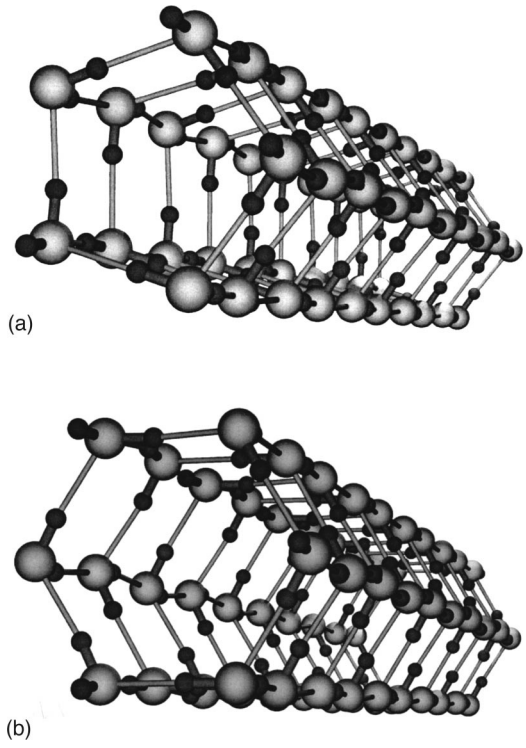

FIG. 1. A lateral cut of pentagon and hexagon ice nanotubes with ABAB-stacking (Ref. 4) results in a finite-size (a) pentagon and (b) hexagon water cluster, respectively. Big and small spheres represent oxygens and hydrogens, respectively, and the long thinner bonds denote the hydrogen bonding.

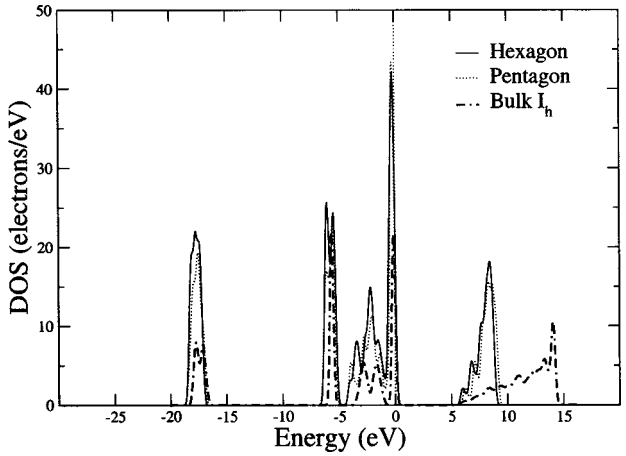

FIG. 2. Electronic density of states (DOS) of Q1D hexagon ice nanotube (solid line), pentagon ice nanotube (dotted line), and proton-ordered bulk ice I_h (dash-dotted line).

functional is treated in the Perdew–Wang (PW91)[11] generalized-gradient approximation (GGA). The wave functions are expanded by using a plane wave basis set with a kinetic energy cutoff of 450 eV. The ion-valence electron interactions are represented by ultrasoft pseudopotential.[12] The Brillouin zone was sampled with $(1\times1\times5)$ k points of a Monkhorst–Pack grid.[13] Because the hexagon and pentagon ice nanotubes are Q1D, the supercell geometry is taken to be a tetragonal cell with the dimension $L\times L\times L_z$ where the z direction is chosen to be the axial direction of the ice nanotubes. We used a 10-molecule supercell for pentagon and a 12-molecule supercell for hexagon ice nanotube. The two water layers in the supercell were chosen to be the ABAB-stacking[4] (Fig. 1). Thus, L_z is just $2a_z$ where a_z is the mean lattice constant of the Q1D ice in the z direction. In the calculations, L was chosen to be 20 Å. The CASTEP code allows full geometry optimization for Q1D periodic systems, i.e., L_z is allowed to vary to achieve the zero-pressure condition in the axial direction. The energy criterion for geometry optimization is 5×10^{-6} eV/molecule. The final optimized value of L_z is 5.672 Å, corresponding to the minimized energy of -471.5501 eV/molecule for hexagon ice nanotube. Those for the pentagon ice nanotube are 5.557 Å and -471.4386 eV/molecule, respectively. Hence, the GGA calculation indicates that the hexagon ice nanotube is slightly more stable than the pentagon ice nanotube; the energy difference is 0.1115 eV/molecule or 10.76 kJ/mol.

We also independently examined the relative stability of the hexagon and pentagon ice nanotubes using the Vienna *ab initio* simulation package (VASP).[14] In this case, the exchange-correlation functional was treated in the local-density approximation (LDA) with the Ceperley–Alder potential[15] based on quantum Monte Carlo simulations. Kinetic energy cutoff is taken to be 395.7 eV. The Brillouin zone was sampled with $(1\times1\times8)$ k points of a Monkhorst–Pack grid. Again, the supercell contains 10 molecules for pentagon ice nanotube and 12 molecule for hexagon ice nanotube. We used 20 Å$\times$20 Å$\times L_z$ supercell size. The energy criterion for geometry optimization was set at 10^{-4} eV/supercell. The optimized value of L_z is 5.21 Å for both hexagon and pentagon ice nanotubes, both are slightly smaller than those obtained from the GGA calculation. It is known that LDA generally overbinds water molecules,[16] which leads to a smaller a_z. Moreover, in contrast to the GGA calculation, the minimized energy for pentagon ice nanotube is actually lower than that for hexagon ice nanotube, but the energy difference is merely 0.0012 eV/molecule. That the prediction of the relative stability between the two Q1D polmorphs are opposite on the basis of GGA and LDA suggests that the two ice polymorphs may be nearly isoenergetic. To summarize, two independent *ab initio* calculations show that the Q1D pentagon and hexagon ice nanotubes are metastable phases of ice at 0 K in vacuum since 3D bulk ice is expected to be the more stable phase at this condition. However, the Q1D ice nanotubes can become a stable phase relative to other confined Q1D phases in a hydrophobic pore with a diameter about 1 nm.[6] The van der Waals attraction between the the confined water and the wall, although weak in comparison with the hydrogen bonding interaction, can further stabilize the Q1D ice nanotubes relative to other 3D bulk phases so that the confined Q1D ice can be in equilibrium with a bulk phase (e.g., liquid water).[7]

Figure 2 displays the calculated electron density of states (DOS) for both hexagon and pentagon ice nanotubes. For comparison, the DOS of proton-ordered bulk ice I_h is also shown in Fig. 2. The DOS calculation was based on PW91 GGA within the DFT. The Fermi energy was set at zero. Interestingly, we find that the Q1D ice nanotubes have the nearly same value of the energy bandgap, $E_g\approx5$ eV, as that of the bulk ice I_h. Note that the optical absorption experiments[17,18] have shown that the absorption edge which

corresponds to the energy bandgap, E_g, is 7.8 eV for proton-disordered ice I_h. Our calculated DOS for the bulk ice I_h is in very good agreement with a previous theoretical calculation of electron energy spectrum for the proton-disordered ice I_h.[19] In that work, the tight-binding approach was used for which a hopping matrix element was adjusted to fit the experimental bandgap 7.8 eV. For bulk ice I_h both calculations show that the DOS has a few singularity-like peaks due to the high degrees of degeneration at these values of energy.[19] In addition to the bandgap, we find the two Q1D ice nanotubes show nearly the same electron energy spectrum as that of ice I_h except some small difference in fine peaks. We therefore tentatively conclude that the overall DOS features appear to be not very sensitive to the local hydrogen-bonding structure so long as the entire molecular system has long-range positional order.

The fine electronic structural differences between the pentagon and hexagon ice nanotubes and the bulk ice I_h can be shown by using the Mulliken population analysis. For bulk ice I_h, it is found that the Mulliken charge is $0.49e$ for H and $-0.98e$ for O. In the case of pentagon ice nanotube, however, O still has a charge $-0.98e$ as that of ice I_h, but H exhibits two different charges, $0.51e$ for in-plane H or $0.47e$ for H involved in hydrogen bonding in the axial direction. The calculated electron density distribution also showed that the hydrogen bonds in the plane of pentagon exhibit a slightly denser electron density than that for the hydrogen bonds in the axial direction. Finally, in the case hexagon ice nanotube, a variety of Mulliken charges on O and H sites was found. In fact, H has eight different charges ranging from $0.47e$ to $0.53e$ while O has two charges, $-1.00e$ or $-1.01e$. This result indicates that the O–O–O angles in the hexagon ice nanotube deviate appreciably from the tetrahedral angle 109.47°, and thus gives rise to a quite different electronic distribution compared to that of pentagon ice nanotube.

In addition to the pseudopotential total-energy calculation for the Q1D ices, we also performed large-scale quantum-chemistry calculations to examine energetics of finite-size pentagon and hexagon water clusters consisting of 30, 60, and 120 molecules. Clusters of this kind[20] can serve to bridge the gap between the small polygonal water rings[21,22] and the infinitely long Q1D polygon ice nanotubes. Both molecular-orbital and density-functional methods (implemented in GAUSSIAN 98 software package)[23] were employed. The water clusters were generated from a lateral cut of the Q1D ice nanotubes. Thus, these clusters are either pentagonal or hexagonal prisms (see Fig. 1). The geometries of the pentagon and hexagon water clusters $(H_2O)_{30}$, $(H_2O)_{60}$, and $(H_2O)_{120}$ were fully optimized using the B3LYP/6-31+G(d), B3LYP/6-31G, and HF/6-31G levels of theory, respectively. The geometries of the optimized clusters were then used for single-point energy calculation at the HF/6-31G(d,p) level for all clusters. At this level, the number of basis amounted to about 3000 for $(H_2O)_{120}$. Furthermore, the correlation corrections were evaluated at the MP2/6-31G(d) level, but only for the smaller $(H_2O)_{30}$ and $(H_2O)_{60}$ clusters.

Single-point energy calculations at the HF/6-31G(d,p) level show that the pentagon water clusters are energetically more stable than the hexagon water clusters. Figure 3 shows that the energy difference per molecule versus the size of the clusters. For $(H_2O)_{30}$ the hexagon cluster is 0.244 kJ/mol less stable than the pentagon one. For the $(H_2O)_{60}$ and $(H_2O)_{120}$ the energy difference increases to 0.370 kJ/mol and 0.346 kJ/mol, respectively. The latter result indicates that the relative energy difference begins to decrease for the water clusters with the size $(H_2O)_{120}$. Zero-point vibration energy difference was also calculated for the two $(H_2O)_{30}$ clusters, which is 0.0251 kJ/mol. Although the hexagon water cluster has a slightly lower zero-point vibration energy, the difference is about one order of magnitude smaller than the single-point energy difference between pentagon and hexagon water clusters. Thus, at the HF/6-31G(d,p) level the pentagon water clusters are more stable than the hexagon water clusters. At the MP2/6-31G(d) level, the energy calculations also indicated that the pentagon water clusters are more stable than the hexagon water clusters. For $(H_2O)_{30}$ the hexagon cluster is higher in energy by 0.370 kJ/mol, whereas for $(H_2O)_{60}$ the hexagon cluster is higher by 0.908 kJ/mol. The correlation correction at the MP2 level increases the relative energy difference between the pentagon and hexagon water clusters, but the qualitative results obtained at the Hartree–Fock level are not changed. For infinitely long Q1D ice nanotubes, on the other hand, our *ab initio* pseudopotential total-energy calculations suggest that the pentagon and hexagon ice nanotubes are likely isoenergetic. We therefore conclude that one can start to see the relative energetic behavior of "bulk" Q1D ice for polygon water prisms at the size $(H_2O)_{120}$.

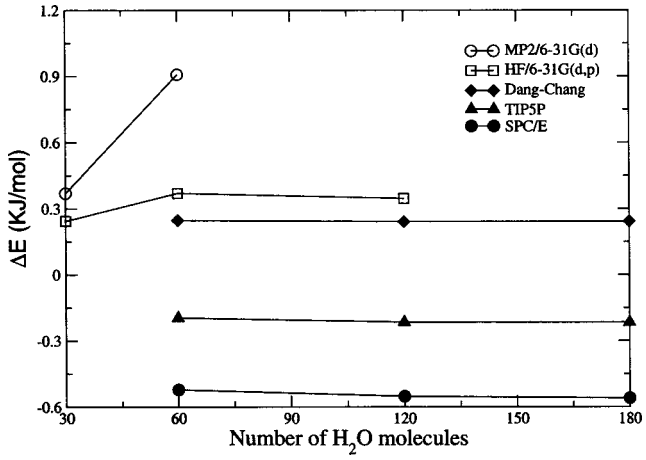

FIG. 3. Energy difference (per molecule) $\Delta E = E_{hex} - E_{pen}$ vs the number of H_2O molecules in hexagon and pentagon water clusters.

Finally, we examined the relative stability of three hexagon and pentagon water clusters [$(H_2O)_{60}$, $(H_2O)_{120}$ and $(H_2O)_{180}$] by using three additional potential models of water: TIP5P,[24] SPC/E,[25] and Dang–Chang polarizable models.[26] The optimized structures for every water model were obtained with the steepest-descent method. Zero-point vibration energy[4,27] was evaluated using normal-mode analysis, but only for TIP5P and SPC/E models. The vibration energy was then added to the potential energy of the corresponding optimized water cluster structure. Figure 3 also displays the energy difference between hexagon and pentagon

water clusters for all three models of water, respectively. For both nonpolarizable models (TIP5P and SPC/E), the hexagon clusters were predicted to be more stable than the pentagon clusters. However, with the Dang–Chang polarizable model, the pentagon clusters were predicted to be slightly more stable, in agreement to the prediction based on the all-electron quantum-chemistry calculation. We thus conclude that the inclusion of polarizibility in the water model appears to be important in predicting the relative stability of large water clusters.

One of the authors (X.C.Z.) is grateful for valuable discussions with Professor Ken Jordan and Professor Guang-Tu Gao. This work is supported by the U.S. NSF, by the NSFC and Chinese Ministry of Education and Ministry of Science and Technology, and by the JSPS and Japan Ministry of Education. Part of the computation was performed on Research Computing Facility at the University of Nebraska-Lincoln.

[1] M. C. Payne, M. P. Teter, D. C. Allen, T. A. Arias, and J. D. Joamopolous, Rev. Mod. Phys. **64**, 1045 (1992); D. K. Remler and P. A. Madden, Mol. Phys. **70**, 921 (1990).
[2] C. Lee, D. Vanderbilt, K. Laasonen, R. Car, and M. Parrinello, Phys. Rev. Lett. **69**, 462 (1992).
[3] A. F. Goncharov, V. V. Struzhkin, M. S. Somayazulu, R. J. Hemley, and H. K. Mao, Science **273**, 218 (1996); K. Aoki, H. Yamawaki, M. Sakashita, and H. Fujihisa, Phys. Rev. B **54**, 15673 (1996); Ph. Pruzan, E. Wolanin, M. Gauthier, J. C. Chervin, B. Canny, and D. Häusermann, J. Phys. Chem. B **101**, 6230 (1997).
[4] K. Koga, R. D. Parra, H. Tanaka, and X. C. Zeng, J. Chem. Phys. **113**, 5037 (2000).
[5] K. Karapetian and K. D. Jordan, unpublished results on molecular mechanics study of TIP4P ice in carbon nanotubes at 0 K.
[6] K. Koga, G. T. Gao, H. Tanaka, and X. C. Zeng, Nature (London) **412**, 802 (2001).
[7] K. Koga, G. T. Gao, H. Tanaka, and X. C. Zeng, Physica A **314**, 462 (2002).
[8] W. L. Jorgensen, J. Chandrasekhar, J. D. Madura, R. W. Impey, and M. L. Klein, J. Chem. Phys. **79**, 926 (1983).
[9] Y. Maniwa, H. Kataura, M. Abe, S. Suzuki, Y. Achiba, H. Kira, and K. Matsuda, J. Phys. Soc. Jpn. (in press).
[10] The CASTEP software code is distributed and maintained by Accelyrs Inc.
[11] J. P. Perdew and Y. Wang, Phys. Rev. B **46**, 12947 (1992).
[12] D. Vanderbilt, Phys. Rev. B **41**, 7892 (1990).
[13] H. J. Monkhorst and J. D. Pack, Phys. Rev. B **13**, 5188 (1976).
[14] G. Kresse and J. Hafner, Phys. Rev. B **47**, 558 (1993); G. Kresse and J. Furthmüller, *ibid.* **54**, 11169 (1996).
[15] D. M. Ceperley and B. J. Alder, Phys. Rev. Lett. **45**, 566 (1980).
[16] D. R. Hamann, Phys. Rev. B **55**, R10157 (1997).
[17] M. Seki, K. Kobayashi, and J. Hakahara, J. Phys. Soc. Jpn. **50**, 2643 (1981).
[18] K. Kobayashi, J. Phys. Chem. **87**, 4317 (1983).
[19] V. F. Petrenko and I. A. Ryzhkin, Phys. Rev. Lett. **71**, 2626 (1993).
[20] C. J. Tsai and K. D. Jordan, J. Phys. Chem. **97**, 5208 (1993).
[21] K. Kim, K. D. Jordan, and T. S. Zwier, J. Am. Chem. Soc. **116**, 11568 (1994).
[22] K. Liu, J. D. Cruzan, and R. J. Saykally, Science **271**, 929 (1996).
[23] M. J. Frisch *et al.*, GAUSSIAN 98, Revision A.9, Gaussian, Inc. Pittsburgh, PA, 1998.
[24] M. W. Mahoney and W. L. Jorgensen, J. Chem. Phys. **112**, 8910 (2000).
[25] H. J. C. Brendsen, J. R. Griegera, and T. P. Straatsma, J. Phys. Chem. **91**, 6269 (1987).
[26] L. X. Dang and T. M. Chang, J. Chem. Phys. **106**, 8149 (1997).
[27] A. Pohorille, L. R. Pratt, R. A. LaViolette, M. A. Wilson, and M. A. MacEroy, J. Chem. Phys. **87**, 6070 (1987).